The structure of two manganese hexacyanometallates(II): $Mn_2[Fe(CN)_6].8H_2O$ and $Mn_2[Os(CN)_6].8H_2O$

A. Gómez
Institute of Materials and Reagents, University of Havana, San Lazaro and L, 10400 Havana, Cuba

V. H. Lara and P. Bosch
Universidad Autonoma Metropolitana, Unidad Iztapalapa, México D.F., México

E. Reguera[a]
Institute of Materials and Reagents, University of Havana, San Lazaro and L, 10400 Havana, Cuba

The crystal structures of two manganese hexacyanometallates(II), $Mn_2[Fe(CN)_6].8H_2O$ and $Mn_2[Os(CN)_6].8H_2O$, were refined from X-ray powder diffraction data using the Rietveld method, with the reported structure for $Mn_2[Ru(CN)_6].8H_2O$ used as a structural model. These compounds are isomorphous and crystallize in the monoclinic space group $P2_1/n$. Their crystallization water is not firmly bound and can be removed without disrupting the $M-C\equiv N-Mn$ network. In the dehydrated complexes, the outer cation (Mn) remains linked to only three N atoms from CN ligands while the inner cation (Fe,Os) preserves its coordination sphere. The IR, Raman, and Mössbauer spectra for the hydrated and anhydrous forms are explained based on the refined structures. © *2002 International Centre for Diffraction Data.* [DOI: 10.1154/1.1469023]

I. INTRODUCTION

Transition metal hexacyanometallates(II), $T_2[M^{II}(CN)_6].xH_2O$, where T is a transition metal, are known to crystallize in cubic space group $F43m$ (Rigamonti, 1937; Rigamonti, 1938; Ratuszna *et al.*, 1995). These crystal structures are highly symmetric, with all cyanide groups linking metal centers in a three-dimensional framework. The outer metal (T) is located in two independent crystallographic sites: one of them coordinated to six cyanide groups through N, while the other one is in the middle of the cubic cavity formed by the framework. Such an arrangement, in which $-T-N\equiv C-M-C\equiv N-T-$ connections are typical, has been reported for Co, Ni, and Cu hexacyanoferrates(II) (Rigamonti, 1937; Rigamonti, 1938; Ratuszna *et al.*, 1995). Manganese hexacyanoruthenate(II), however, crystallizes in a different space group ($P2_1/n$), in which $-Ru-C\equiv N-Mn-(H_2O)_2-Mn-N\equiv C-$ bridges are observed; two neighbor manganese atoms are linked by two water molecules (Ruegg *et al.*, 1971). Such a structure is expected to have interesting absorption properties when dehydrated. Manganous ferrocyanide and osmocyanide have been reported as being isomorphous to the ruthenium complex; their structures, however, have not been reported (Reguera *et al.*, 2001). The present study deals with the structural refinement of these two complexes. Since no single crystals were available, their structures were refined using the Rietveld method complemented with IR, Raman, and Mössbauer spectroscopies.

II. EXPERIMENTAL

Manganese ferrocyanide was prepared by mixing aqueous solutions of manganese chloride and ferrocyanic acid. The precipitated solid was washed several times with distilled water and dried in a desiccator over silica gel. Manganese osmocyanide was prepared in the same manner but using potassium hexacyanoosmate(II). In this paper these compounds are abbreviated Mn_2Fe^{II} and Mn_2Os^{II}. The stoichiometry suggested by these abbreviations was checked by X-ray fluorescence analysis. Their hydration degree was determined using thermogravimetry.

IR spectra were recorded in the range $4000-400\ cm^{-1}$ using the KBr disk technique and a Fourier transform infrared spectrometer (ATI Mattson, Genesis Series). Raman spectra were obtained using a 1403 Spex double monochromator in the frequency range of $1900-2400\ cm^{-1}$. Mössbauer spectra were collected at room temperature with a ^{57}Co in Rh source, using a constant acceleration spectrometer (from Mostech) operated in the transmission mode. All Mössbauer spectra were fitted with an iterative least-squares minimization algorithm using pseudo-Lorentzian line shapes to obtain the values of isomer shift (δ), quadrupole splitting (Δ), linewidth (Γ), and relative area (A). Isomer shift values are reported relative to sodium nitroprusside.

X-ray diffraction (XRD) powder patterns were obtained with a Siemens D5000 diffractometer with a graphite monochromator and Cu$K\alpha$ radiation ($\lambda = 0.154\ 183\ 8$ nm). Patterns were taken in the interval from 10° to 100° (2θ) with a step size of 0.03° and a counting time of 20 s. Since preferred orientation was observed when the samples were pressed into the diffractometer sample holder, the powder was ground in an agate mortar and then suspended in acetone, which was rapidly dried over a glass sample holder. This procedure eliminated the preferred orientation, so that

[a] Author to whom correspondence should be addressed; electronic mail: edilso@ff.oc.uh.cu

TABLE I. Details of the refinement of the structures: $Mn_2[Fe(CN)_6].8H_2O$ and $Mn_2[Os(CN)_6].8H_2O$.

	$Mn_2[Fe(CN)_6].8H_2O$	$Mn_2[Os(CN)_6].8H_2O$
Data collection		
Diffractometer	Siemens D5000	Siemens D5000
Monochromator	Graphite	Graphite
Wavelength (Å)	Cu $K\alpha$1 1.540 562	Cu $K\alpha$1 1.540 562
	Cu $K\alpha$2 1.544 390	Cu $K\alpha$2 1.544 390
2θ range	10–100°	10–100°
Step size	0.03°	0.03°
Time per step (s)	20	20
Unit cell		
Space group	$P2_1/n$	$P2_1/n$
a (Å)	9.3656 (5)	9.4922 (7)
b (Å)	12.2731 (7)	12.4930 (7)
c (Å)	7.4816 (4)	7.6013 (6)
β (°)	98.649 (3)	98.695 (5)
Refinement		
Number of observations	3001	3001
Number of contributing reflections	884	921
Number of distance constraints	6	6
Number of refined parameters		
Structural parameters	37	37
Profile parameters	11	11
R_{exp}	10.4	7.62
R_{wp}	12.6	10.1
R_B	8.76	6.62
S	1.21	1.32

the refinement proceeded smoothly without refining preferred orientation parameters.

Rietveld refinement was performed using the program FULLPROF (Rodriguez-Carvajal, 1996) taking as an initial model the structure of manganese hexacyanoruthenate (Ruegg *et al.*, 1971). In the two cases the distances within the hexacyanometallate(II) anion were constrained to the ones observed in the structures of related compounds (Herren *et al.*, 1980; Baraldo *et al.*, 1994). The variation in the constrained distances was only allowed within the reported error. Removal of these constraints resulted in less satisfactory distances and angles without any improvement in the profile fit, so they were retained. In Table I are reported details of the refinement process. Figure 1 shows the experimental XRD powder patterns, the calculated patterns, and their differences.

III. RESULTS AND DISCUSSION

A. Refined structure

Both $Mn_2[Fe(CN)_6].8H_2O$ and $Mn_2[Os(CN)_6].8H_2O$ are isomorphous and crystallize in the space group $P2_1/n$. The observed differences in cell parameters (see Table I) are expected due to differences in the ionic radii of Fe(II) and Os(II). In Tables II, III, IV are presented the atomic coordinates, the bond distances, and the bond angles, respectively. The inner cation (Fe or Os) is sited on an inversion center and has the usual octahedral coordination to six cyanide C atoms, forming slightly distorted octahedra (see Table IV).

The manganese atoms coordinate in an unusual way to three nitrogen atoms of the cyanide groups and three water-
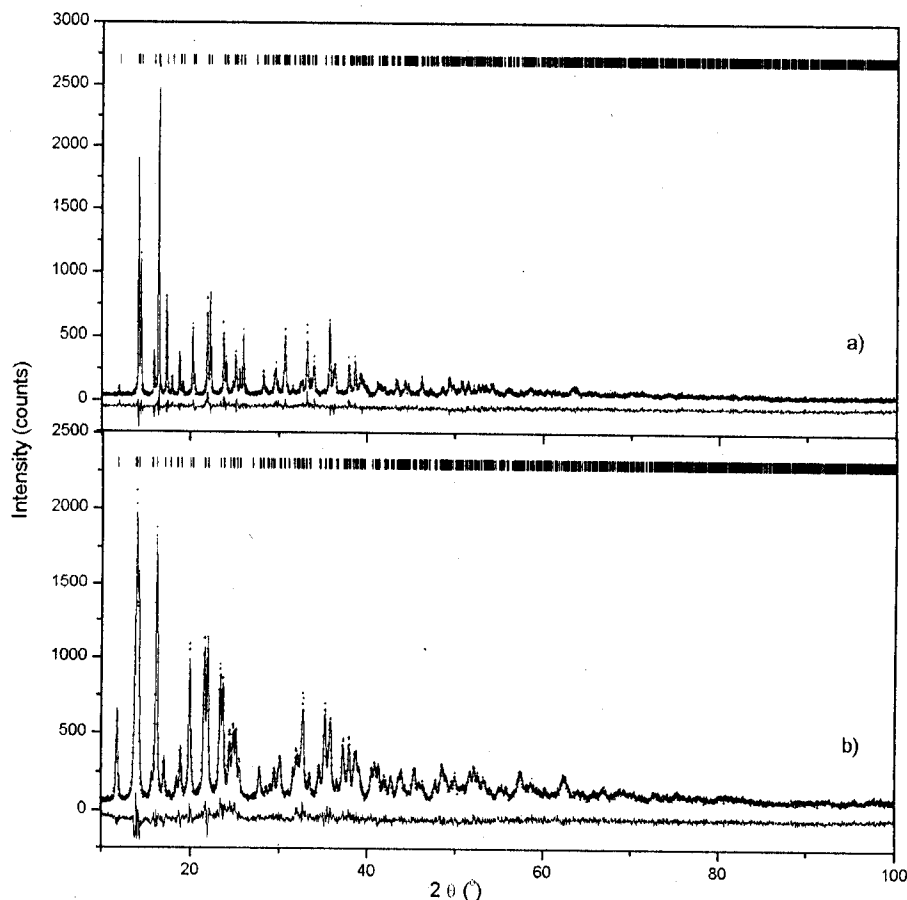

Figure 1. XRD powder patterns of: (a) $Mn_2[Fe^{II}(CN)_6].8H_2O$ and (b) $Mn_2[Os^{II}(CN)_6].8H_2O$. Observed (points), calculated (line), and difference profiles (lower trace) are from the Rietveld refinement. The vertical markers at the top show the positions calculated for the Bragg reflections.

TABLE II. Atomic positions for: (a) $Mn_2[Fe(CN)_6].8H_2O$ and (b) $Mn_2[Os(CN)_6].8H_2O$.

	x	y	z	Biso
(a)				
Fe	0.5	0.5	0.5	1.1(2)
Mn	0.6301(5)	0.094 7(4)	0.4235(7)	1.4(2)
C1	0.579(2)	0.358 6(10)	0.473(3)	1.2(3)
C2	0.627(2)	0.554 6(15)	0.344(3)	1.2(3)
C3	0.359(2)	0.467 7(16)	0.294(2)	1.2(3)
N1	0.620(2)	0.269 4(9)	0.466(2)	1.2(3)
N2	0.7115(17)	0.585 4(14)	0.255(2)	1.2(3)
N3	0.2685(15)	0.444 6(14)	0.174(2)	1.2(3)
O1	0.4502(16)	0.096 2(12)	0.183(2)	2.2(3)
O2	0.4253(15)	0.092 8(12)	0.585(2)	2.2(3)
O3	0.2376(16)	0.229 7(12)	0.403(2)	2.2(3)
O4	0.9598(16)	0.292 2(13)	0.385(2)	2.2(3)
(b)				
Os	0.5	0.5	0.5	1.04(2)
Mn	0.6264(7)	0.095 2(5)	0.4230(10)	1.08(2)
C1	0.583(2)	0.347 9(15)	0.479(2)	1.41(3)
C2	0.636(2)	0.556 4(16)	0.336(3)	1.41(3)
C3	0.3495(14)	0.465 5(12)	0.281(2)	1.41(3)
N1	0.625(2)	0.263 0(9)	0.466(2)	1.41(3)
N2	0.715(2)	0.585 9(18)	0.244(2)	1.41(3)
N3	0.2614(18)	0.444 5(19)	0.165(2)	1.41(3)
O1	0.457(2)	0.094 0(17)	0.188(3)	1.91(3)
O2	0.421(2)	0.087 3(17)	0.579(3)	1.91(3)
O3	0.230(3)	0.226 74(19)	0.409(3)	1.91(3)
O4	0.965(3)	0.299 5(17)	0.400(3)	1.91(3)

TABLE IV. Bond angles for $Mn_2[Fe(CN)_6].8H_2O$ and $Mn_2[Os(CN)_6].8H_2O$.

	$Mn_2[Fe(CN)_6].8H_2O$	$Mn_2[Os(CN)_6].8H_2O$
C1–M–C2	88.1(1.3)	89.2(1.3)
C1–M–C3	87.8(1.3)	88.3(1.1)
C2–M–C3	90.0(1.5)	90.1(1.2)
N1–Mn–N2	101.2(1.1)	99.7(1.2)
N1–Mn–N3	97.3(1.0)	96.6(1.2)
N1–Mn–O1	93.7(9)	96.3(1.4)
N1–Mn–O2	83.1(8)	86.7(1.2)
N1–Mn–O2'	162.4(1.0)	164.8(1.4)
N2–Mn–N3	98.4(1.1)	96.8(1.1)
N2–Mn–O1	90.4(1.0)	90.5(1.4)
N2–Mn–O2	170.8(1.2)	170.5(1.7)
N2–Mn–O2'	95.8(1.0)	95.5(1.4)
N3–Mn–O1	164.2(1.2)	163.9(1.8)
N3–Mn–O2	89.0(9)	89.4(1.3)
N3–Mn–O2'	84.6(9)	82.5(1.3)
O1–Mn–O2	81.1(9)	81.7(1.5)
O1–Mn–O2'	81.5(9)	82.6(1.4)
O2–Mn–O2'	79.4(8)	78.1(1.3)
M–C1–N1	174.3(1.4)	178.1(1.6)
M–C2–N2	176.0(1.9)	178.0(2.0)
M–C3–N3	176.5(1.7)	176.3(1.8)
Mn–N1–C1	163.6(1.4)	160.2(1.9)
Mn–N2–C2	164(2)	164(2)
Mn–N3–C3	170.4(1.8)	170.0(1.8)
Mn–O2–Mn'	100.6(6)	101.8(9)

molecules, which form very distorted octahedra with N1–Mn–N2 and O2–Mn–O2' angles around 100° and 79°, respectively (see Table IV). That distortion is also evident from the N2–Mn–N3 and O1–Mn–O2' angles, which are close to 98° and 81°, respectively (see Figure 2). In cubic hexacyanides the M–C≡N angle is 180°; in the studied compounds, however, M–C1≡N1, M–C2≡N2, and M–C3≡N3 angles are in the range from 174° to 178° in order to reduce the asymmetry in the inner metal environment.

TABLE III. Bond distances for $Mn_2Fe(CN)_6.8H_2O$ and $Mn_2Os(CN)_6.8H_2O$.

	$Mn_2[Fe(CN)_6].8H_2O$	$Mn_2[Os(CN)_6].8H_2O$
M–C1	1.910(14)	2.072(19)
M–C2	1.91(2)	2.050(19)
M–C3	1.916(18)	2.070(16)
Mn–N1	2.172(12)	2.122(13)
Mn–N2	2.145(17)	2.115(19)
Mn–N3	2.166(15)	2.137(18)
Mn–O1	2.272(16)	2.21(3)
Mn–O2	2.416(16)	2.43(2)
Mn–O2	2.359(16)	2.32(2)
C1–N1	1.163(18)	1.14(2)
C2–N2	1.17(3)	1.16(3)
C3–N3	1.17(2)	1.15(2)
O1–O4	2.63(2)	2.57(3)
O2–O3	2.65(2)	2.70(3)
O2–O4	2.63(2)	2.80(3)
O3–O4	2.70(2)	2.66(4)
Mn–Mn'	3.673(7)	3.693(10)
O2–O2'	3.05(2)	3.00(3)

The Mn–Mn bridges, not observed in cubic complexes, are formed in these structures as a consequence of two water molecules being shared by two neighboring manganese atoms. As a result, two edge sharing octahedra are obtained, forming the moiety: $Mn_2N_6(H_2O)_4$. In this way, the unusual M–C≡N–Mn$(H_2O)_2$–Mn–N≡C–M linkage alternates with the usual Mn–N≡C–M one (see Figure 2). Zeolitic water molecules are also observed in the structure; they are sited in small channels in the structure and are hydrogen bonded to coordinated water molecules. Coordinated water molecules that link Mn atoms do not interact through hydrogen bonding, since they are very distant (at 3.0 Å) and their O atoms participate as ligands of Mn.

The water in the studied complexes is not firmly bonded, even the coordinated molecules. When these compounds are heated, they lose water from about 80 °C and become anhydrous at 140 °C. The anhydrous complex does not show the XRD pattern corresponding to the hydrated form, but this is restored when the sample rehydrates, indicating that the dehydration process does not affect the M–C≡N–Mn skeleton. These complexes have a relatively open structure with channels of about 3.9×4.5 Å. Removing coordinated water increases the channel size. In these conditions the Mn atoms remain coordinated to only three N atoms and could behave as an active site to coordinate certain chemical species that could be introduced through the channels.

B. IR and Raman spectra

IR spectra of the studied compounds are very simple, with three absorption bands associated with the CN ligands [ν(CN), δ(M–C≡N), and ν(M–C)] and seven absorption bands due to coordinated and uncoordinated water [ν(O–H),
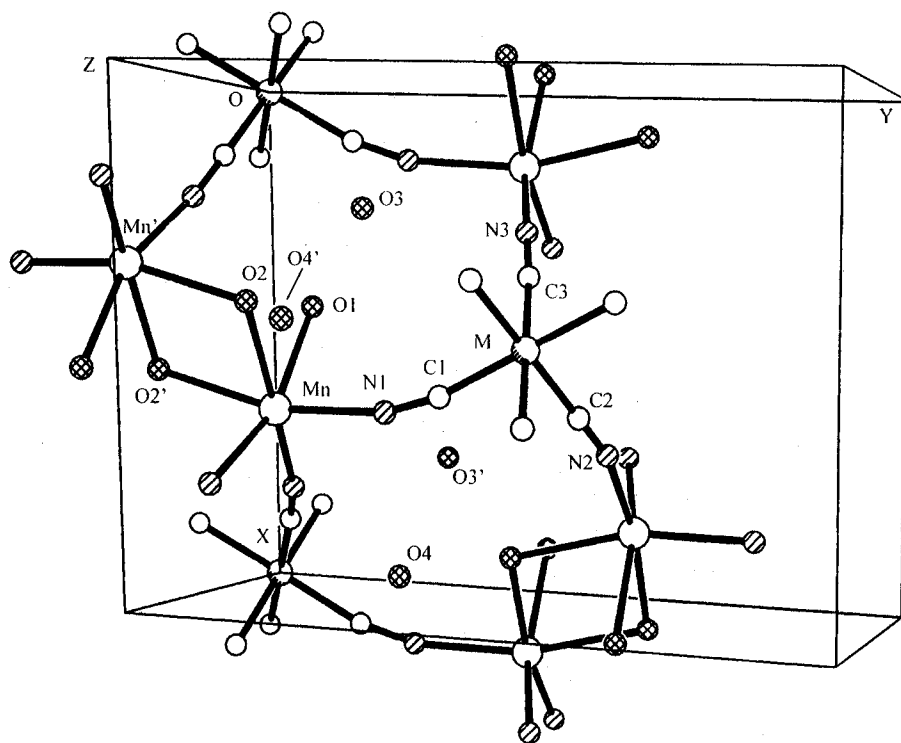
Figure 2. View of the structure of $Mn_2[Fe^{II}(CN)_6].8H_2O$ along the Z axis showing $Mn_2N_6(H_2O)_4$ sharing octahedra. Two water molecules are bridging two Mn atoms (O2) while the other two remain as solely bound to that metal (O1).

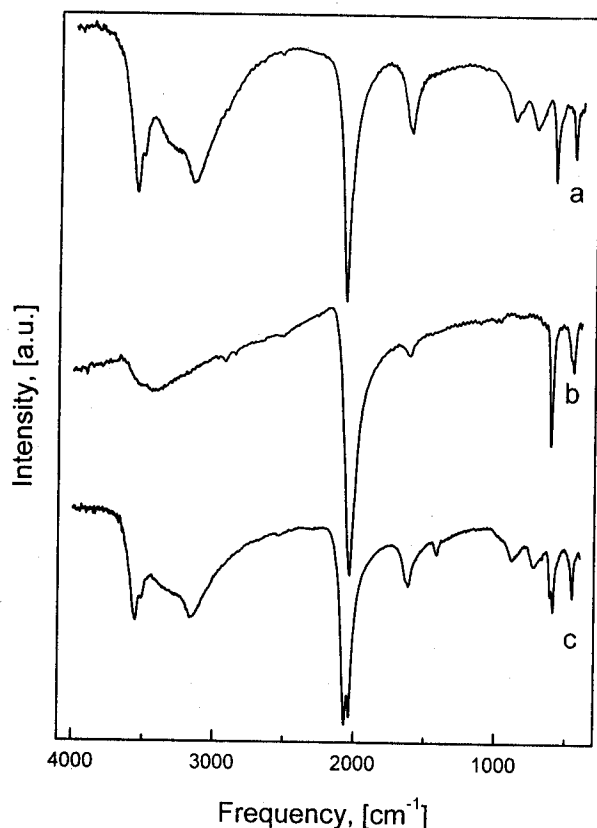Figure 3. IR spectra of: (a) $Mn_2[Fe^{II}(CN)_6].8H_2O$; (b) $Mn_2[Fe^{II}(CN)_6].0H_2O$; (c) $Mn_2[Fe^{II}(CN)_6].xH_2O$ ($x<8$) partially rehydrated. Indicated is the assignment of the observed absorption bands. The bands in the 800–700 cm^{-1} region (ρ_r and w) correspond to the rocking and wagging vibration modes of the water molecules that link the Mn atoms. On dehydration these IR bands disappear and CN stretching bands shift to the low frequency zone.

δ(H–O–H), ρ_r(H$_2$O) and w(H$_2$O)], see Figure 3 and Table V. The stretching vibration of the CN ligands appears as a single absorption indicating that all C≡N bonds are equivalent, as was supposed in the refinement process. The Raman modes E_g and A_{1g} also are single absorptions at 2088 and 2127 cm^{-1}, respectively. The δ(M–C≡N) and ν(M–C) vibrations are observed in the expected frequency values for hexacyanometallates (II) (Nakamoto, 1997). There are four absorption bands that can be assigned to coordinated water: the two narrow bands at 3560 and 3515 cm^{-1}, and the rocking and wagging vibrations at 820 and 701 cm^{-1}. These last two bands correspond to the water molecules that are bridging Mn atoms. The broad stretching bands in the region 3350–3150 cm^{-1} are due to zeolitic water.

When the complexes are heated to 140 °C, the absorption bands due to coordinated and uncoordinated water disappear. IR and Raman spectra of the dehydrated compounds correspond to hexacyanometallates indicating that the dehydration process does not affect the M–C≡N–Mn network

TABLE V. Infrared frequencies, in cm^{-1}, for $Mn_2[Fe(CN)_6].8H_2O$ and $Mn_2[Os(CN)_6].8H_2O$.

$Mn_2[Fe(CN)_6].8H_2O$	$Mn_2[Os(CN)_6].8H_2O$	Assignment
3561	3573	O–H(ν), coord. H$_2$O
3516	3521	O–H(ν), coord. H$_2$O
3297 (br)[a]	3336 (br)	O–H(ν), uncoordinated
3150 (br)[a]	3205 (br)	water
2071	2071	C≡N(ν)
1622	1616	H–O–H(δ)
883	827	H$_2$O(rocking)
730	699	H$_2$O(wagging)
591	550	M–C≡N(δ)
456	456	M–C(ν)

[a]br: broad band.
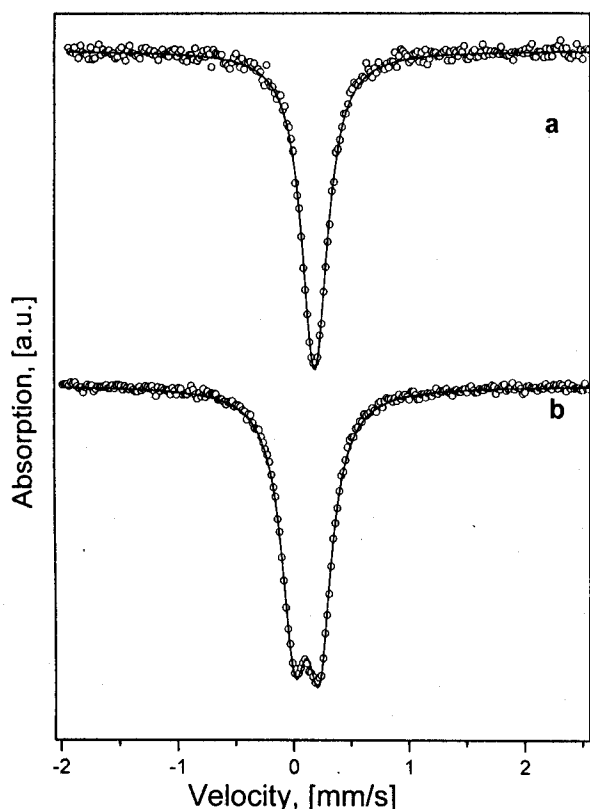
Figure 4. Mössbauer spectra at room temperature of: (a) $Mn_2[Fe^{II}(CN)_6].8H_2O$; (b) $Mn_2[Fe^{II}(CN)_6].0H_2O$. The breaking of the water bridges that connect Mn atoms induces a remarkable π back donation effect that is observed as a decrease in the isomer shift value.

electrons are taken from the iron cation, the shielding of s electrons at the nucleus decreases and the value of δ also decreases. Higher s electron density at the iron nucleus results in a lower isomer shift value (Gutlich, 1975). The observed value of the quadrupole splitting for the anhydrous complex is a result of a pronounced distortion in the environment of the iron complex. The loss of coordinated water affects the equilibrium of forces in the network and it induces an additional deformation in the iron neighborhood.

IV. CONCLUSIONS

The structures of $Mn_2[Fe(CN)_6].8H_2O$ and $Mn_2[Os(CN)_6].8H_2O$ were refined using the Rietveld method, with the reported structure for $Mn_2[Ru(CN)_6].8H_2O$ as a starting model. The crystallization water in these complexes is not firmly bound and can be removed without disrupting the M–C≡N–Mn network. In the dehydrated complexes, the outer cation (Mn) remains linked to only three N atoms of the CN ligands.

ACKNOWLEDGMENT

[see Figures 3(b) and 3(b′)]. In the dehydrated form the outer cation (Mn) remains coordinated by only three N atoms from CN ligands. In these conditions manganese increases its interaction with the CN ligands mainly through a σ mechanism. To compensate for that effect the CN ligands take more electrons from the inner metal (Fe, Os) through a π back bonding mechanism, weakening the C≡N bond. As a result of these combined effects the CN stretching vibration shifts to a lower frequency [Figure 3(b) and Table IV]. The observed shift in ν(CN) (IR) is about 32 cm⁻¹. The corresponding Raman modes, E_g and A_{1g}, now absorb at 2053 and 2109 cm⁻¹, respectively. A minor but significant change is also observed in the δ(M–C≡N) vibration (see Table V).

C. Mössbauer spectra

The Mössbauer spectrum of $Mn_2[Fe(CN)_6].8H_2O$ is a single absorption line, with an isomer shift of 0.184 mm/s, a value typical of low-spin iron (II) (Reguera et al., 1992). The observed linewidth is 0.260 mm/s, which indicates a low asymmetry around the iron cation since no quadrupole interaction due to lattice contribution is detected. When the complex is dehydrated, the observed Mössbauer absorption is a quadrupole doublet ($\Delta = 0.282$ mm/s) with a very low isomer shift (0.072 mm/s). The previously discussed π back bonding weakening the C≡N bond is now observed as a decrease in the value of the isomer shift (Figure 4). When d

Baraldo, L. M., Bessega, M. S., Rigotti, G. E., and Olabe, J. A. (**1994**). "Crystal and molecular structure, spectroscopic properties, and electrophilic reactivity of sodium pentacyanonitrosylosmate(II) dihydrate," Inorg. Chim. Acta **33**, 5890–5896.

Gutlich P. (**1975**). Mössbauer Spectroscopy, 1st ed., edited by U. Gonser (Springer, New York), 402 pp.

Herren, F., Fisher, P., Ludi, A., and Haelg, W. (**1980**). "Neutron diffraction study of Prussian Blue, $Fe_4(Fe(CN)_6)_3$ $(H_2O)_x$. Location of water molecules and long-range magnetic order," Inorg. Chem. **19**, 956–959.

Nakamoto, K. (**1997**). Infrared and Raman Spectra of Inorganic and Coordination Compounds, Applications in Coordination, Organometallic, and Bioinorganic Chemistry, 5th ed. (Wiley, New York), 500 pp.

Ratuszna, A., Juszczyk, S., and Malecki, G. (**1995**). "Crystal structure of the three-dimensional magnetic network of type $MeK(Fe(CN)_6)1.m(H_2O)$, where Me=Cu, Ni, Co," Powder Diffr. **10**, 300–305.

Reguera, E., Fernández, J., Dago, A., and Díaz, C. (**1992**). "Mössbauer study of Prussian Blue from different provenances," Hyperfine Interact. **73**, 295–305.

Reguera, E., Gómez, A., Balmaseda, J., Contreras, G., and Escamilla, A. (**2001**). "Structural characterization of cadmium hexacyanometallates(II) and related complexes," Struct. Chem. **12**, 59–67.

Rigamonti, R. (**1937**). "Struttura dei cupriferrocianuri.-Nota 1. Ferrocianuro di rame e ferrocianuri di rame e potassio," Gazz. Chim. Ital. **67**, 137–146.

Rigamonti, R. (**1938**). "Struttura e costituzione chimica di alcuni ferrocianuri," Gazz. Chim. Ital. **68**, 803–809.

Rodriguez-Carvajal, J. (**1996**). "Program FULLPROF (Version 3.1d-Jul.'96), based on the original code provided by Wiles, D. B., Young, R. A. and Sakthivel, A.," Laboratoire Leon Brillouin (CEA-CNRS), Saclay, France.

Rueg, M., Ludi, A., and Rieder, K. (**1971**). "The crystal structure of manganese (II) hexacyanoruthenate (II) octahydrate, $Mn_2[Ru(CN)_6].8H_2O$," Inorg. Chem. **10**, 1775–1777.